IV

Publication IV

Deposited dielectrics on metal thin films using silicon and glass substrates for hot electron-induced electrochemiluminescence

Antti J. Niskanen [a,b,*], Tiina Ylinen-Hinkka [c], Matti Pusa [c], Sakari Kulmala [c], Sami Franssila [a]

[a] Department of Materials Science and Engineering, Aalto University School of Science and Technology, P.O. Box 16200, FI-00076 Aalto, Finland
[b] Department of Micro and Nanosciences, Aalto University School of Science and Technology, P.O. Box 13500, FI-00076 Aalto, Finland
[c] Laboratory of Analytical Chemistry, Aalto University School of Science and Technology, P.O. Box 16100, FI-00076 Aalto, Finland

ARTICLE INFO

ABSTRACT

Electrochemiluminescence by tunnel emission of hot electrons into aqueous solution is a sensitive method for detection of luminophores e.g. rare-earth chelates, which may be used as labels in bioassays. Electrons are injected into solution from an insulating film-coated working electrode, working against a platinum counter electrode. Conductive silicon electrodes with various tunnel dielectric materials e.g. thermal oxide have been used in previous work. In this paper we explore the use of metal thin film electrodes on silicon and glass substrates, using tunneling dielectrics of aluminum oxide and silicon dioxide made by the low-temperature processes of atomic layer deposition or plasma-enhanced chemical vapor deposition.

© 2010 Elsevier B.V. All rights reserved.

1. Introduction

Electrochemiluminescence based on hot or solvated electrons in aqueous solution is a sensitive and selective method for detecting various luminophores such as luminol [1], fluorescein [2], and other organic luminophores and rare-earth chelates [3]. Detection limits as low as picomolar levels can be attained by spectral discrimination and time-resolved detection [1,4]. Hot electrons can be tunnel emitted into the solution by pulse polarization from conductive electrodes covered by a thin insulating film [5,6]. This tunneling is analogous to tunnel emission of electrons into vacuum [7].

Hot electron-induced electrochemiluminescence (HECL) can also be used as a sensitive detection method in immunoassays by binding specific antibodies to the surface of the working electrode. Antigens in the sample solution can then be detected by a competitive immuno-assay using labeled antigens [8], or by allowing the antigen to bind to the electrode, followed by binding labeled secondary antibodies to the antigens [9].

Highly conductive silicon has previously been used as the sub-strate material of the working electrode, with various tunneling dielectrics including silicon dioxide, silicon nitride and aluminum oxide, deposited by thermal oxidation, low pressure chemical vapor deposition, plasma enhanced chemical vapor deposition (PECVD) and

atomic layer deposition (ALD) being examined [10]. In this work, glass substrates are used in addition to silicon, and thin film working electrodes of deposited metals including aluminum, tungsten, chromium, titanium, platinum and copper are investigated. The dielectric layer is either aluminum oxide deposited by ALD, or silicon dioxide deposited by PECVD. Both are low-temperature processes compatible with metals and glass substrates.

2. Experimental

2.1. Fabrication of the working electrodes

n-type silicon wafers of (111) orientation and 0.005–0.018 Ω cm resistivity were cleaned by a standard RCA-cleaning process comprising 10 min in SC-1 ($NH_4OH + H_2O_2$ solution at 80 °C), 30 s in dilute HF at room temperature and 15 min in SC-2 ($HCl + H_2O_2$ solution at 80 °C). Finally the wafers were stripped of their native oxide with dilute HF. Pyrex glass substrates were cleaned with SC-1 only. The following metal thin films were deposited with an Oxford PlasmaLab 400 sputtering system: 120 nm aluminum, 50 nm platinum, 40 nm titanium, 60 nm tungsten, 50 nm chromium and 200 nm copper. Copper and platinum films had an in-situ deposited 10 nm chromium layer underneath to promote adhesion to the substrate.

The thin film electrodes were coated with various thicknesses of alumina or silicon dioxide. Alumina was deposited by ALD in a Beneq TFS-500 reactor using 10 to 1000 growth cycles of either trimethy-laluminum (TMA) and water, or TMA and ozone. The deposition

temperature was 220 °C and pressure approximately 5 mbar (500 Pa). Silicon dioxide was deposited by PECVD in an Oxford PlasmaLab 80 Plus single-wafer reactor at 300 °C temperature and 1000 mTorr (130 Pa) pressure with 5 W RF power. The reactant gases were SiH_4 (flow rate 2.0 sccm), N_2O (710 sccm) and N_2 (161.5 sccm), and deposition times ranged from 15 to 70 s. Native oxide was wet etched off bare silicon samples immediately prior to deposition, whereas metal samples were used in their natural state as sputtered.

Dielectric thickness was monitored on the metal films as well as on reference samples of bare silicon with a Philips SD 2300 ellipsometer at a wavelength of 632.8 nm, using bulk refractive index values of 1.465 for SiO_2 and 1.766 for Al_2O_3.

2.2. HECL measurements

HECL measurements were made in a round sample cell of 5.6 mm diameter. Electrical contact to the working electrode was made from the wafer backside for silicon samples, or directly to the metal thin film for samples on a glass substrate. The electrode was pulsed using a custom made coulostatic pulse generator at a rate of 20 Hz, as detailed in [11]. The pulse voltage was 25 V and charge 12.6 microcoulombs. After each pulse, and following a 50 microseconds delay, luminescence was measured with a photomultiplier tube during 6 ms. Luminescence data was recorded from a total of 1000 pulses for each sample. Terbium (III) 2,6-bis[N,N-bis(carboxymethyl)amino-methyl]-4-benzoylphenol chelate was used as the model luminophore.

3. Results

3.1. Dielectric deposition on various substrates

ALD of alumina nominally exhibits a deposition rate of about 0.08 nm per growth cycle due to the self-limiting nature of the process [12]. The deposition rate is nearly identical regardless of the oxygen precursor used (ozone or water). The PECVD recipe for silicon dioxide, on the other hand, was specially tailored to yield a lower than normal deposition rate by lowering the RF power and SiH_4 flow. A deposition rate of about 16 nm/min was measured on bare silicon samples.

All samples were measured by ellipsometry after deposition. Growth was confirmed to be linear, with an identical deposition rate over most metals. Only tungsten exhibited a slightly higher growth rate (about 0.11 nm per cycle) in the ALD process, suggesting that in addition to the deposition of alumina on the top surface, unwanted oxidation of tungsten occurs at the metal/dielectric interface. Copper samples, on the other hand, became severely discolored in both deposition processes, and no realistic ellipsometer results were obtained. Surface oxidation is therefore a more plausible explanation than deposition.

Another difference between various electrode materials was an offset in dielectric film thickness, which was independent of the deposition time. Ideally, identical deposition times should produce identical films on all substrates. However, in some samples, especially aluminum, the measured thickness was slightly too high, indicating the presence of a native oxide, or oxidation of the metal surface prior to deposition, *i.e.* during loading of the sample into the reactor. Other samples, especially platinum and chromium, exhibited thinner films than expected, *i.e.* deposition was delayed. In the shortest deposition processes, some of these samples exhibited no deposition at all. After the onset of deposition, however, the deposition rate was identical to the other samples.

This effect of either native oxide formation or delayed deposition is quantified in Table 1 for the various electrode materials. Thickness data after different deposition times has been extrapolated to zero deposition time (or zero deposition cycles in the case of ALD), and this result is termed *thickness offset*. Thus positive offset values correspond

Table 1
Deposited film thicknesses on various electrode materials extrapolated to zero deposition time. Positive values indicate a native oxide or oxidation during sample loading, negative values indicate a corresponding delay in the onset of deposition.

Metal	Thickness offset (nm)		
	Al_2O_3 ALD		SiO_2 PECVD
	TMA/H_2O	TMA/O_3	
Al	+3.2	+5.0	+0.6
Si	+1.7	+3.2	−2.0
W	+0.7	+3.0	−2.0
Ti	−0.8	N/A	−6.8
Pt	−2.3	N/A	−4.2
Cr	−4.3	−1.4	−11.4

to the native oxide thickness prior to deposition, whereas negative values indicate delayed deposition. Since all thicknesses were measured by ellipsometry using the deposited film's bulk refractive index, the actual physical thickness of a native oxide under the deposited film may differ from these results. The PECVD data also reflect the plasma ignition delay specific to the reactor. (Titanium and platinum were unfortunately not available at the time of the TMA/O_3 ALD tests. Copper is not included in the table, as no deposition occurred on any samples.)

3.2. HECL performance of deposited films

Figs. 1 and 2 present the observed HECL signal as a function of ALD alumina thickness using aluminum, platinum and tungsten thin film electrodes, as well as bulk silicon electrodes, with alumina deposited by TMA/H_2O and TMA/O_3 processes. The model analyte was a 10^{-6} mol/dm^3 solution of Tb(III) chelate. Chromium, titanium and copper data are not included, as they did not produce any significant HECL signal. The data are integrated over the entire 1000 pulse measurement. An optimum film thickness in the range of 4–10 nm is evident for most electrode materials, the ozone deposition process being obviously more critical regarding thickness.

Fig. 3 shows the photon counts from successive measurement pulses. This depicts the stability of the ALD alumina covered electrode over the course of the measurement. These results were measured from dielectrics deposited with the TMA/H_2O process. The TMA/O_3 results were similar. While platinum electrodes initially give a higher intensity, they stop working soon after 100 pulses, thus producing the lower integrated intensity seen in Fig. 1. Tungsten electrodes break down even sooner. However, both silicon and aluminum electrodes are much more stable. Extended measurements demonstrated that Al/Al_2O_3 electrodes withstand at least 40 000 pulses with a gradual
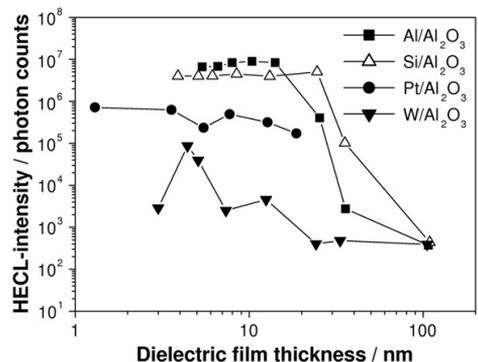

Fig. 1. HECL signal versus dielectric film thickness using ALD Al_2O_3 dielectric deposited from TMA and water.
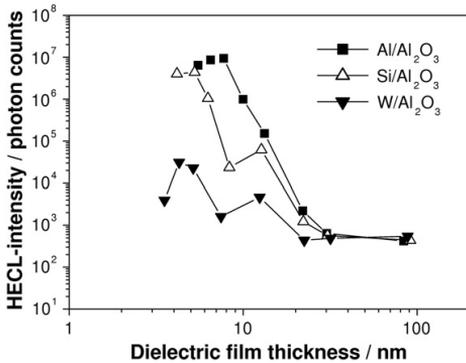
Fig. 2. HECL signal versus dielectric film thickness using ALD Al_2O_3 dielectric deposited from TMA and ozone.
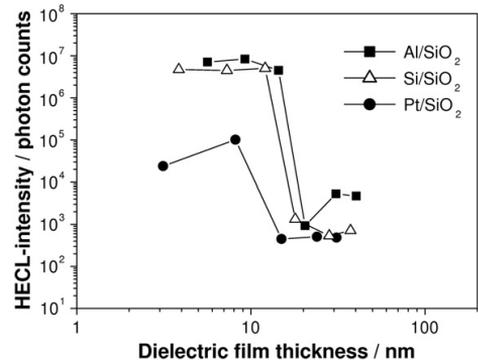

Fig. 4. HECL signal versus dielectric film thickness using PECVD SiO_2 dielectric.

decrease in signal (25% decrease using the TMA/O_3 process, only 5% using the TMA/H_2O process, initial and final intensities integrated over 4000 pulses). Si/Al_2O_3 using TMA/O_3 perform well over 10 000 pulses with about 10% fluctuation in intensity before breakdown.

Tunneling dielectrics deposited with PECVD yielded quite similar results as ALD, albeit tungsten electrodes produced virtually no signal. The thickness optimum is around 4–10 nm, falling very rapidly after that. Silicon electrodes with a PECVD dielectric were stable up to 4000 pulses, after which the HECL intensity fell abruptly. Aluminum electrodes with a PECVD dielectric were measured to be stable to 40 000 pulses with a gradual decrease in intensity of about 25% from beginning to end. Figs. 4 and 5 present the thickness dependence and stability of PECVD SiO_2 dielectric over aluminum, platinum and silicon. Other metals did not produce significant HECL and are therefore not included.

The shelf life of HECL working electrodes is good. No degradation has been observed in electrodes up to 10 months old, when stored in normal laboratory room air.

4. Discussion

Deposited dielectrics over metal thin film electrodes were shown to work well as tunnel emitter electrodes in HECL applications, with good signal intensity and stability. The exceptional stability of the aluminum working electrodes may be due to self-healing of any defects formed during operation. The rapid oxidation of bare aluminum surfaces in either water or air is well known, and aluminum electrodes covered by nothing but a native oxide have also been found

to work [2]. The importance of the electrode metal is obvious, as the performance of two completely different deposition processes (ALD and PECVD) gave such similar results: excellent stability over silicon and aluminum, lesser stability over platinum or tungsten, and no signal on the other metals tested.

The poor performance of certain metals in this HECL application exhibits a strong correspondence with the observed deposition delays in ALD and PECVD on that metal (Table 1). Due to poor growth initiation, the overall quality of the deposited film may be worse close to the metal/dielectric interface, leading to breakdown of the dielectric when voltage is applied. Delayed deposition could also be expected to initiate growth as individual disconnected islands, resulting in a non-uniform thickness of the film. By the time the film has become continuous and sufficiently thick in the delayed areas, much of the surface area would then already be too thick for optimal HECL efficiency.

To check for such island-type growth, atomic force microscope (AFM) measurements were made of platinum and chromium samples after various ALD deposition times. An NT-MDT NTegra scanning probe microscope was used in contact mode with a 10 nm radius silicon tip. Fig. 6 shows the surface topography of a platinum electrode as sputtered, and after 20 and 70 ALD cycles in the TMA/H_2O process. Neither an island structure, nor an increase in surface roughness, is evident from the AFM images. Rather, the smoothing and broadening of surface grains, and the unchanged vertical range of the images, are consistent with conformal deposition. In addition, an island-type growth should also have produced a lower ellipsometrically observed growth rate in the early stages of deposition, since ellipsometry
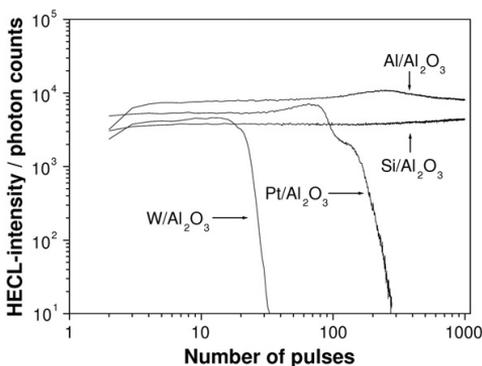

Fig. 3. HECL signal of successive measurement pulses using ALD AL_2O_3 film of optimal thickness (TMA/H_2O process).
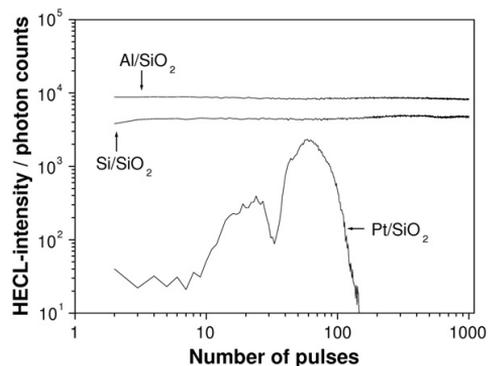

Fig. 5. HECL signal of successive measurement pulses using PECVD SiO_2 film of optimal thickness.
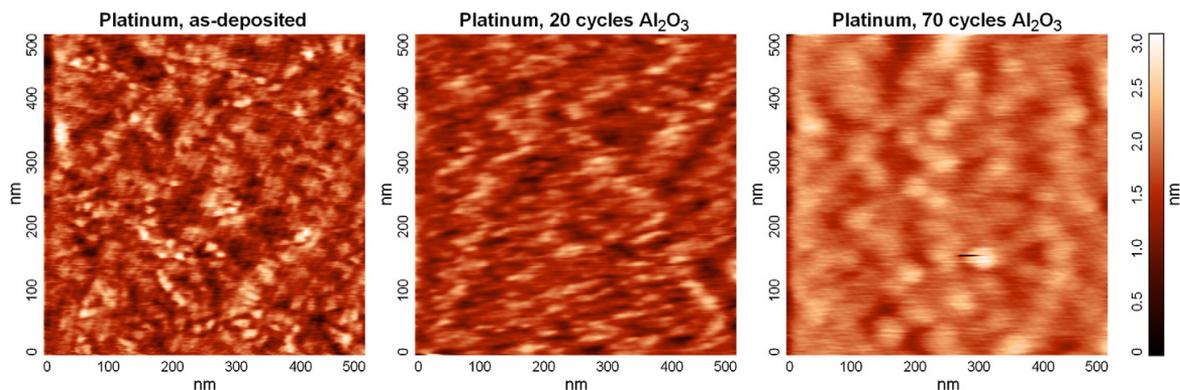
Fig. 6. Surface topography of a platinum electrode with 0, 20 and 70 cycles of deposited Al_2O_3. The vertical (z) scale is the same in all three images.

effectively averages film thickness over the laser spot area. Instead, growth rates remained constant immediately after the onset of deposition.

In terms of HECL performance, the main outlier is tungsten, which exhibits a positive thickness offset in ALD and a relatively small negative offset in PECVD, and should therefore be expected to perform better as a tunnel dielectric. However, as the higher observed deposition rate over tungsten suggests, the metal is likely being oxidized at the metal/dielectric interface. This would result in a non-uniform dielectric structure containing oxides of tungsten as well as alumina or silica. Copper electrodes, as well, clearly oxidized on their surface during loading into the reactor. They exhibited no deposition at all of either alumina or silica, and therefore did not work as HECL electrodes.

The difference in optimal film thickness for HECL between alumina dielectrics produced by TMA/H_2O and TMA/O_3 ALD processes is notable. The optimal dielectric thickness over a silicon electrode is drastically lower for the ozone process, and a significant difference is also seen over aluminum (Figs. 1 and 2). Since ozone is a more aggressive oxidant than water [13], it is likely to produce a denser alumina film. The ozone process has also been demonstrated to leave less residual carbon in the bulk of the film, and to produce less aluminum sub-oxides near the substrate interface [14]. Especially on a bare hydrogen-terminated n^+ silicon surface, as was used in this work, aluminum clusters may be formed at the Si/Al_2O_3 interface in the TMA/H_2O process [15]. The use of ozone as the oxidant precursor suppresses these clusters, and also avoids OH radical contamination of the film, leading to reduced leakage currents in capacitor dielectrics [16]. Our observations are in line with these reported effects. OH radical and carbon contamination likely plays a significant role, since differences were seen in both silicon and aluminum electrodes, but the drastic difference in silicon may be attributable to aluminum cluster formation.

Despite these differences between the TMA/H_2O and TMA/O_3 processes, both types of alumina dielectrics worked equally well in the HECL application. The difference was evident only in the thickness required for optimal HECL performance, as well as the difference in thickness offsets (Table 1) which were consistently more positive in the TMA/O_3 process, as would be expected from a more aggressive precursor.

5. Conclusions

The performance of HECL working electrodes comprising deposited metal thin films covered by deposited tunnel dielectrics was shown to be comparable to that of thermally oxidized silicon or anodized aluminum electrodes used in previous work [10,11]. Of the tested metals, the most suitable for deposited HECL electrodes were aluminum and platinum, the former offering high signal intensity and excellent stability over thousands of measurement pulses.

While thermal oxidation of silicon and anodization of aluminum [17] are both well controlled and convenient processes for manufacturing the working electrodes, a deposited dielectric has the benefit of being independent of substrate material. If the metal electrode is also deposited in thin film form, non-conductive substrates can be used. The deposition processes used here are relatively low temperature processes, which widens the possibilities of HECL device fabrication to cheap glass or even plastic substrates, as well as the possibility to integrate other sensors or electronics on the same chip. PECVD silicon dioxide, ALD alumina, and possibly a wide variety of other dielectrics can be chosen for a given application according to their chemical resistance or antibody binding properties.

References

[1] J. Suomi, M. Håkansson, Q. Jiang, M. Kotiranta, M. Helin, A.J. Niskanen, S. Kulmala, Anal. Chim. Acta 541 (2005) 167.
[2] T. Ylinen, J. Suomi, M. Helin, T. Ala-Kleme, S. Kulmala, J. Fluoresc. 16 (2006) 27.
[3] S. Kulmala, M. Helin, T. Ala-Kleme, L. Väre, D. Papkovsky, T. Korpela, A. Kulmala, Anal. Chim. Acta 386 (1999) 1.
[4] M. Håkansson, Q. Jiang, M. Helin, M. Putkonen, A.J. Niskanen, S. Pahlberg, T. Ala-Kleme, L. Heikkilä, J. Suomi, S. Kulmala, Electrochim. Acta 51 (2005) 289.
[5] S. Kulmala, T. Ala-Kleme, L. Heikkilä, L. Väre, J. Chem. Soc. Faraday Trans. 93 (1997) 3107.
[6] S. Kulmala, T. Ala-Kleme, H. Joela, A. Kulmala, J. Radioanal. Nucl. Chem. 232 (1998) 91.
[7] C.A. Mead, J. Appl. Phys. 32 (1960) 646.
[8] J. Eskola, P. Mäkinen, L. Oksa, K. Loikas, M. Nauma, Q. Jiang, M. Håkansson, J. Suomi, S. Kulmala, J. Lumin. 118 (2006) 238.
[9] T. Ala-Kleme, P. Mäkinen, T. Ylinen, L. Väre, S. Kulmala, P. Ihalainen, J. Peltonen, Anal. Chem. 78 (2006) 82.
[10] A.J. Niskanen, T. Ylinen-Hinkka, S. Kulmala, S. Franssila, Thin Solid Films 517 (2009) 5779.
[11] S. Kulmala, M. Håkansson, A.-M. Spehar, A. Nyman, J. Kankare, K. Loikas, T. Ala-Kleme, J. Eskola, Anal. Chim. Acta 458 (2002) 271.
[12] S.M. George, A.W. Ott, J.W. Klaus, J. Phys. Chem. 100 (1996) 13121.
[13] K. Grigoras, S. Franssila, V.-M. Airaksinen, Thin Solid Films 516 (2008) 5551.
[14] S. Jakschik, U. Schroeder, T. Hecht, D. Krueger, G. Dollinger, A. Bergmaier, C. Luhmann, J.W. Bartha, Appl. Surf. Sci. 211 (2003) 352.
[15] W.S. Yang, Y.K. Kim, S.-Y. Yang, J.H. Choi, H.S. Park, S.I. Lee, J.-B. Yoo, Surf. Coat. Technol. 131 (2000) 79.
[16] J.B. Kim, D.R. Kwon, K. Chakrabarti, C. Lee, J. Appl. Phys. 92 (2002) 6739.
[17] J.W. Diggle, T.C. Downie, C.W. Goulding, Chem. Rev. 69 (1969) 365.